Journal of Materials Chemistry C

ROYAL SOCIETY OF CHEMISTRY

PAPER

View Article Online
View Journal | View Issue

Cite this: J. Mater. Chem. C, 2023, 11, 8929

Tuning the rare-earth UiO-66 metal–organic framework platform for white light emission†

Zvart Ajoyan,‡[ab] Hudson A. Bicalho,‡[ab] P. Rafael Donnarumma,[ab] Artsiom Antanovich[c] and Ashlee J. Howarth *[ab]

Received 5th April 2023,
Accepted 6th June 2023

DOI: 10.1039/d3tc01199b

rsc.li/materials-c

Metal–organic frameworks (MOFs) have received notable attention owing to their structural diversity, permanent porosity, and high surface areas. In addition to these properties, MOFs made of rare-earth (RE) metals have the potential to be used in photoluminescent applications, where photoluminescence is dictated by the identity of the metal ion and organic linker that are used to construct the RE-MOF. In this study, we investigate the photoluminescent properties of RE-UiO-66 by synthesizing and characterizing mono-, bi-, and tri-metallic analogues of RE-UiO-66 (RE = Tb(III), Eu(III), and Gd(III)), with the aim of designing a MOF with white light emitting properties. Additionally, as a proof of concept, the new Tb : Gd : Eu-UiO-66 MOF is used as a surface coating on a UV light emitting diode (LED) to give a white light emitting device where photostability of the MOF is tested.

Introduction

The development of energy efficient lighting technologies is important for reducing global electricity consumption, and thus greenhouse gas emissions.[1] As such, the replacement of traditional, low energy efficiency lighting sources such as incandescent and fluorescent lamps, is required for mitigating the global energy crisis.[2] As one of the most promising solutions, light emitting diodes (LEDs) have gained interest due to their relatively long lifespan,[3] high energy efficiency,[4,5] and accessibility to a wide range of colours and temperatures.[6] By tuning the colour and temperature of specific phosphors, white LEDs (WLEDs) can be produced and used for applications in solid state lighting and displays.[4,7]

Currently, there are three popular strategies for the production of WLEDs; (i) utilizing multiple LED chips, where each chip emits red, green, and blue (RGB) light that is mixed to give white,[4] (ii) coating UV-LED chips with phosphors that absorb UV light and emit triple wavelength RGB,[8,9] (iii) coating blue LED chips with phosphors that absorb a portion of blue light, and emit green and red.[4,10] When designing a material for approach ii, the Commission International de l'Eclairage (CIE) chromaticity diagram is often used to determine and compare the colour purity of the RGB emitting phosphor.[11] Two coordinates from the visible region are calculated, where pure white is defined as $x, y = 0.33, 0.33$.

Significant effort has gone into the development of new white light (RGB) emitting materials including the study of organic molecules or polymers,[12,13] metal-doped materials,[14,15] metal complexes,[16] and nanomaterials as phosphors.[17,18] In the solid-state, pure organic molecules and polymers are prone to luminescence quenching, posing a challenge for long term lighting applications.[19] On the other hand, inorganic phosphors have higher efficiencies and longer lifetimes relative to organic phosphors, but often suffer from challenges related to solution processability.[20]

Metal–organic frameworks (MOFs) are a class of coordination polymers that are comprised of inorganic metal nodes and organic linkers, forming 2- or 3-dimensional network structures.[21–26] MOFs have the potential to combine the advantageous properties of both traditional organic and inorganic phosphors. Currently, only a handful of white light emitting MOFs have been reported in the literature,[27–34] with some emitting from the organic component,[27] inorganic component,[35] both metal and organic components,[28–30,36] and others requiring doping with coordination compounds,[31] perovskites,[32] or rare-earth (RE) elements.[37] MOFs comprised of RE elements commonly have trivalent RE ions as part of their metal node, with the nodes separated from each other by organic linkers, preventing self-quenching and photobleaching,[38,39] and thus making RE-MOFs interesting candidates for WLEDs.[40] In particular, RE-MOFs comprised of multinuclear cluster nodes[41] allow for the incorporation of multiple RE ions at high concentrations, but with

[a] Department of Chemistry and Biochemistry and Centre for NanoScience Research, Concordia University, 7141 Sherbrooke Street West, Montréal, Quebec H4B 1R6, Canada. E-mail: ashlee.howarth@concordia.ca
[b] FRQNT Quebec Centre for Advanced Materials (QCAM/CQMF), Montreal, Canada
[c] Department of Physical Chemistry, Technische Universität Dresden, Zellescher Weg 19, 01069, Dresden, Germany

† Electronic supplementary information (ESI) available. CCDC 2265674. For ESI and crystallographic data in CIF or other electronic format see DOI: https://doi.org/10.1039/d3tc01199b

‡ Z. A. and H. A. B. contributed equally to this work

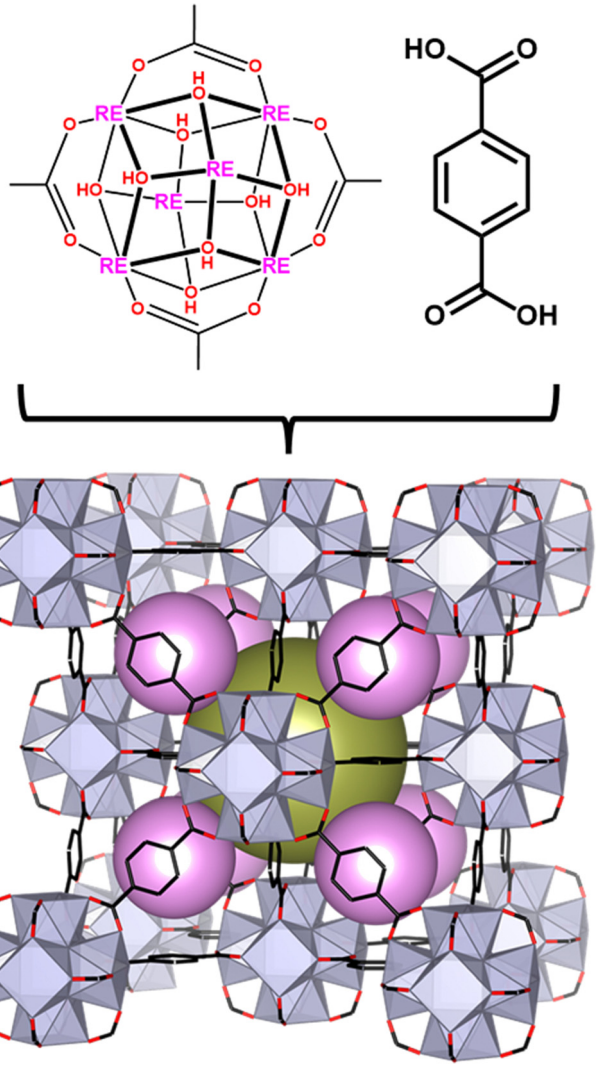

Fig. 1 Structure of RE-UiO-66 depicting the RE_6 cluster with the H_2BDC linker forming the **fcu** net with the tetrahedral cage (pink spheres) and octahedral cage (gold sphere).

ordered separation, giving rise to a high degree of colour tunability in these materials.

The archetypal MOF, Zr-UiO-66, has been reported in numerous studies for its robust structure,[42,43] high surface area,[44,45] and porosity.[46] More recently, we reported RE analogues of UiO-66 comprised of RE_6–cluster nodes bridged by 1,4-benzenedicarboxylate (BDC^{2-}) linkers (Fig. 1).[47] Given that Eu(III) and Tb(III) ions emit red and green light, respectively,[48,49] and BDC^{2-} emits in the blue region,[50] we hypothesized that the RE-UiO-66 platform would be ideal for the design of a white light (RGB) emitting MOF. In addition to emitting blue light, the BDC^{2-} linker in RE-UiO-66 plays a key role in the sensitization of the RE metals *via* the antenna effect.[51–56] Herein, we evaluate the photoluminescent behaviour of mixed metal RE-UiO-66 analogues (RE = Tb(III), Eu(III), and Gd(III)) by tuning the ratio of RE ions to give bi- and tri-metal RE_6–nodes, ultimately leading to the formation of a white light emitting MOF.

Results and discussion

RE-UiO-66 analogues with mono- (Tb(III), Gd(III), Eu(III)), bi- (Gd : Eu, Tb : Gd, Tb : Eu) and tri-metal (Tb : Gd : Eu) nodes are synthesized using a $RE(NO_3)_3{\cdot}xH_2O$ precursor (see Table S1 for details, ESI†) with the ditopic linker H_2BDC in the presence of a fluorinated modulator, 2,6-difluorobenzoic acid (2,6-DFBA), in *N*,*N*-dimethylacetamide (DMA). In order to confirm the bulk crystallinity and phase purity of all mono-, bi-, and tri-metal RE-UiO-66 analogues, powder X-ray diffraction (PXRD) data were collected. As can be observed in Fig. 2a and Fig. S1 (ESI†), all reflections are consistent with the expected **fcu** topology of RE-UiO-66. N_2 adsorption–desorption analysis of bi- and tri-metal RE-UiO-66 show reversible Type I isotherms (Fig. 2b and Fig. S2, ESI†), as expected for RE-UiO-66, with an experimental Brunauer–Emmett–Teller (BET) surface area of 930 $m^2\ g^{-1}$ for the tri-metal Tb : Gd : Eu-UiO-66 analogue (Fig. 2b). Diffuse reflectance infrared Fourier transform spectroscopy (DRIFTS) of Tb : Gd : Eu-UiO-66 confirms the presence of some μ_3-OH and/or terminal –OH groups in the RE_6-cluster nodes (Fig. S3, ESI†), however it should be noted that there is the possibility for μ_3-OH and μ_3-F ligands due to the use of a fluorinated modulator during the MOF synthesis.[57] Indeed, the ^{19}F-NMR spectrum (Fig. S4, ESI†) of a digested sample of Tb : Gd : Eu-UiO-66 displays a peak at approximately −165 ppm. This peak is assigned to HF and has been observed in other cluster-based RE-MOFs containing μ_3-F bridges.[58] Scanning electron microscopy (SEM) micrographs reveal the expected octahedral morphology of Tb : Gd : Eu-UiO-66 with an average crystallite size of 21 μm (Fig. 3). Additionally, energy dispersive X-ray spectroscopy (EDS) shows a homogeneous distribution of Tb(III), Gd(III), and Eu(III) ions (Fig. 3, Fig. S5, ESI†), suggesting that all three RE ions are incorporated in the individual crystallites of the MOF. After several attempts at producing a white light emitting MOF, through systematically varying the ratio of Tb : Gd : Eu, the ideal ratio was found to be 1.5 : 4.1 : 0.4. The incorporation of RE ions in RE-UiO-66 with this molar ratio is confirmed by inductively coupled plasma-mass spectrometry (ICP-MS) (see Table S2 for ICP-MS data on all bi- and tri-metal analogues, ESI†). Finally, to unequivocally confirm the presence of the three RE(III) ions in the tri-metal RE-UiO-66 crystallites, single

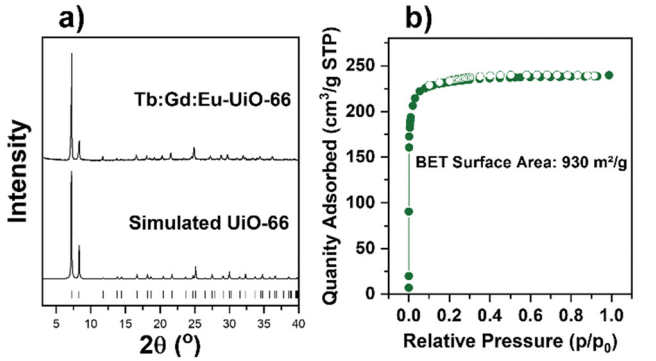

Fig. 2 (a) PXRD pattern of synthesized Tb : Gd : Eu-UiO-66 and the simulated pattern, and (b) nitrogen sorption isotherm of Tb : Gd : Eu-UiO-66.

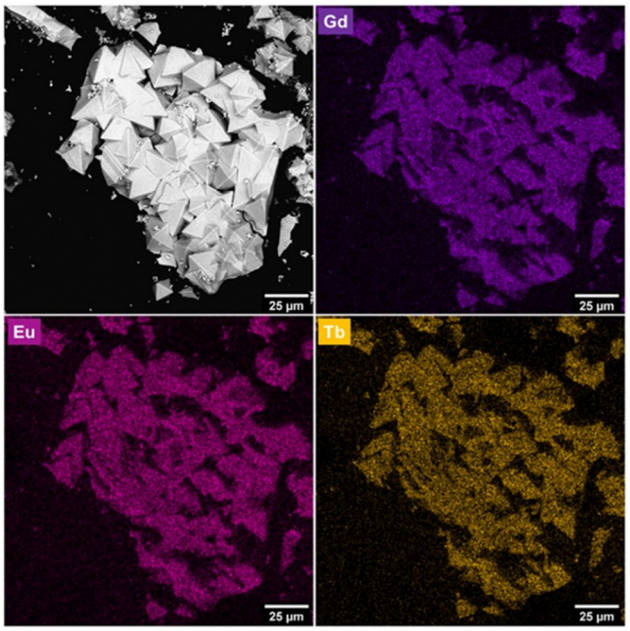

Fig. 3 SEM micrographs and EDS mapping of Gd:Eu:Tb-UiO-66.

crystals of the tri-metal RE-UiO-66 suitable for single crystal X-ray diffraction (SCXRD) were grown and the X-ray diffraction data collected. As can be seen in Fig. S6 (ESI†), upon UV light irradiation, the MOF crystals emit a cool white colour. When the same ratio of Tb : Gd : Eu obtained by ICP-MS was used to solve the crystal structure of tri-metal RE-UiO-66, adequate wR_2 values were obtained (Table S3, ESI†). As such, the combination of white light emission observed from the single crystals (Fig. S5, ESI†) and the crystal structure solution showing acceptable wR_2 values when solved with Tb(III), Gd(III), and Eu(III), further confirms the presence of the three RE(III) ions and the expected ratio of 1.5 : 4.1 : 0.4 for Tb : Gd : Eu.

Eu(III) and Tb(III) ions emit from their $^5D_0$ and $^5D_4$ states, which have energies of 17 250 and 20 500 cm^{-1}, respectively.[59] Tb(III) emission can be sensitized *via* the antenna effect through energy transfer from the triplet excited state (T_1) of an organic ligand to its $^5D_4$ state (20 500 cm^{-1}), whereas Eu(III) emission can be sensitized through energy transfer to its $^5D_0$ state (17 250 cm^{-1}), or higher lying ^5D_J states ($^5D_1$ = 19 000 cm^{-1}, and $^5D_2$ = 21 450 cm^{-1}).[60] As such, sensitization of both Tb(III) and Eu(III) *via* the antenna effect requires a linker with T_1 energy of at least 22 350 cm^{-1} according to Latva's rule.[59,60] If the T_1 energy of the linker is too close to the acceptor state of the lanthanoid, energy back-transfer to the linker can occur, leading to quenching of the lanthanoid emission.[60] Alternatively, if the T_1 energy of the linker is too high (>26 000 cm^{-1}), there will be inefficient energy transfer to the lanthanoid.[61,62] BDC^{2-} has a T_1 energy of 25 641 cm^{-1},[50] which is sufficient for sensitizing both Eu(III) and Tb(III) emission. Given that Eu(III) and Tb(III) ions may be present in the same RE_6-cluster of RE-UiO-66, and therefore 3.92 Å apart, energy transfer from Tb(III) to Eu(III) is also possible.[63] Tb(III) ions give rise to green emission with sharp emission bands at 489, 544, 582 and 617 nm, $^5D_4 \rightarrow {}^7F_{6,5,4,3}$ as can be seen in Tb-UiO-66 (Fig. S7a, ESI†). Eu(III) ions give rise to red emission with sharp emission bands at 590, 615, 655, 696 nm, $^5D_0 \rightarrow {}^7F_{1,2,3,4}$ as can be observed in Eu-UiO-66 (Fig. S7b, ESI†). Eu-UiO-66 also exhibits a broad blue emission with moderate intensity spanning 350–500 nm corresponding to the singlet state (S_1) emission of the BDC^{2-} linker and suggesting that energy transfer from the BDC^{2-} linker to Eu(III) does not occur with 100% efficiency.

In order to increase the contribution of the blue linker emission in RE-UiO-66 to generate a white light emitting MOF, a RE(III) ion with high energy 4f excited states is required to further supress the linker T_1 to RE(III) energy transfer pathway in RE-UiO-66. Given that Gd(III) has very high energy 4f excited states (>32 000 cm^{-1}), strong BDC^{2-} linker emission is observed in Gd-UiO-66, giving rise to a broad band centered at 425 nm in the blue (Fig. S7c, ESI†). The excited state energy, energy transfer pathways, and emissive states in RE-UiO-66 analogues can be visualized in Fig. 4. The BDC^{2-} linker acts as the light harvester, with absorbance spanning 200–400 nm (Fig. S8a, ESI†). When excited into this absorption band, the excited singlet state of the linker is generated. Owing to the presence of heavy RE(III) ions, intersystem crossing (ISC) occurs and gives rise to the T_1 state of BDC^{2-}. This is followed by non-radiative energy transfer, or the antenna effect, from the BDC^{2-} T_1 state to the 4f excited states of RE(III) ions. Owing to the energy of the T_1 state of BDC^{2-}, energy transfer to both Eu(III) and Tb(III) is possible, whereas energy transfer to the 4f states of Gd(III) is not possible.

Working towards a white light emitting (RGB) RE-UiO-66 analogue, bi-metal analogues of the MOF were first studied to gain information about the antenna effect in mixed-metal RE-UiO-66. In Gd:Eu-UiO-66 (Fig. S9a, ESI†), the blue emission (λ_{em} = 350–500 nm) from the linker is more intense than that observed for Eu-UiO-66 (Fig. S7b, ESI†), relative to the Eu(III) emission. This demonstrates that the presence of Gd(III) leads to less efficient energy transfer from the BDC^{2-} linker T_1 state to the Eu(III) $^5D_0$, $^5D_1$ and $^5D_2$ states, in comparison to that observed in Eu-UiO-66. Tb:Gd-UiO-66 (Fig. S9b, ESI†) on the other hand, exhibits the same photoluminescence emission spectrum as Tb-UiO-66 (Fig. S7a, ESI†), meaning that the presence of Gd(III) does not significantly alter the efficiency of

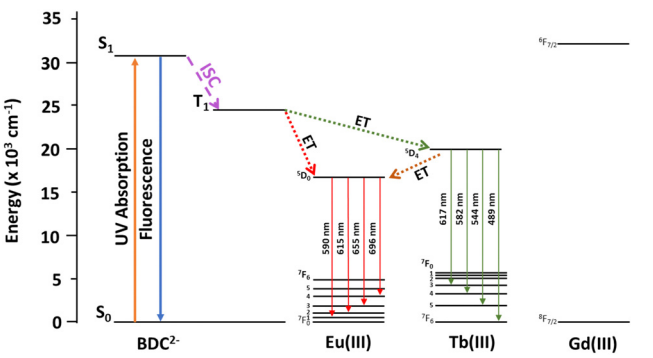

Fig. 4 Jablonski diagram depicting excited state energy levels and the possible energy transfer pathways for the BDC2$^-$ linker and Eu(III), Tb(III), and Gd(III).

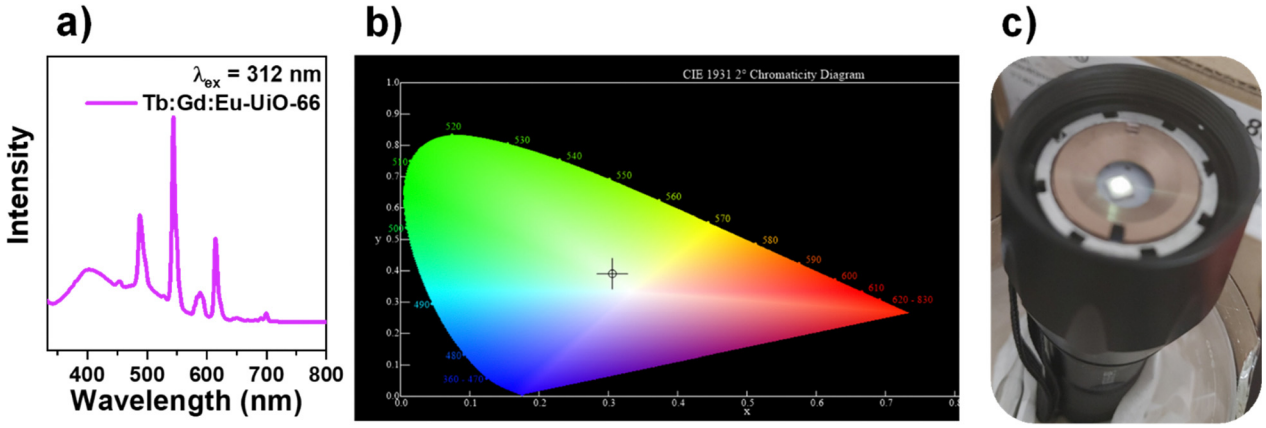

Fig. 5 (a) Photoluminescence emission spectrum of Tb : Gd : Eu-UiO-66, (b) the CIE diagram and (c) Tb : Gd : Eu-UiO-66 on the LED flashlight with UV-LED chip (λ = 310 nm).

energy transfer from the BDC^{2-} linker T_1 state to the Tb(III) $^5D_4$ state. The photoluminescence emission spectrum of Tb:Eu-UiO-66 (Fig. S9c, ESI†) has a weak blue emission (λ_{em} = 350–500 nm) from the linker, in contrast to Tb-UiO-66 and Tb:Gd-UiO-66, which suggests that the addition of Eu(III) decreases the efficiency of energy transfer from the BDC^{2-} linker T_1 state to the Tb(III) $^5D_4$ state, or where it's possible that energy transfer from Tb(III) to Eu(III) might be playing a role. Both Eu(III) and Tb(III) transitions are observed in the emission spectrum of Tb:Eu-UiO-66 with an overlap of the $^5D_4 \rightarrow {}^7F_3$ transition of Tb(III) and $^5D_0 \rightarrow {}^7F_2$ transition of Eu(III), hence displaying emission in the blue, green, and red regions.

Given that green, blue, and red emission is observed in Tb-UiO-66, Gd-UiO-66, and Eu-UiO-66, respectively, as well as in the bi-metal RE-UiO-66 analogues, we reasoned that a judicious mixture of Tb : Gd : Eu should give rise to white light emission. Indeed, the tri-metal RE-UiO-66 analogues composed of Tb(III), Gd(III), and Eu(III) (Tb : Gd : Eu-UiO-66), demonstrate strong blue emission from the linker, narrow green emission from Tb(III), and narrow red emission from Eu(III) (Fig. 5a) when excited into the BDC^{2-} linker at 312 nm (Fig. S8 and S10, ESI†). Tuning the composition of Tb : Gd : Eu to 1.5 : 4.1 : 0.4 in the hexanuclear cluster gives a distribution of green, blue, and red emission simultaneously, giving rise to white-light emission with the CIE 1931 color coordinate of x = 0.3103, y = 0.3901, corresponding to a cool white colour and correlated colour temperature (CCT) of 6287 K (Fig. 5b). Tb : Gd : Eu-UiO-66 shows a quantum yield of 11.4% (Fig. S11, ESI†), similar to that observed for other photoluminescent and white light emitting RE-MOFs.[40,64] Additionally, the trimetallic RE-MOF displays average lifetimes of 22.5 (478 nm), 34.9 (543 nm), and 16.2 μs (613 nm), for the $^5D_4 \rightarrow {}^7F_6$ emission from Tb(III) ions, $^5D_4 \rightarrow {}^7F_5$ emission from Tb(III) ions, and overlapping $^5D_4 \rightarrow {}^7F_3$ emission from Tb(III) ions with $^5D_0 \rightarrow {}^7F_2$ emission from Eu(III) ions, respectively (Fig. S12 and Table S4, ESI†). When compared to the single-metal Tb-UiO-66, which has an emission lifetime on the order of 1000 μs ($^5D_4 \rightarrow {}^7F_5$)[56] the trimetallic Tb : Gd : Eu-UiO-66 displays a lower average lifetime, which suggests energy transfer from Tb(III) to Eu(III) is occurring in the trimetallic MOF.[63,65]

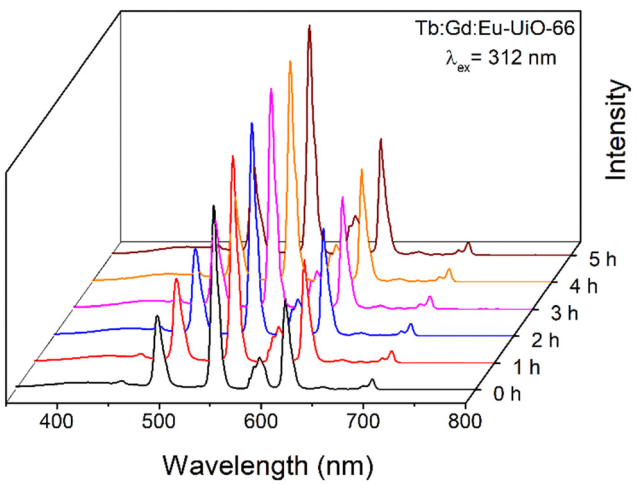

Fig. 6 Photoluminescence emission spectrum of Tb : Gd : Eu-UiO-66 as a function of time under ambient conditions, irradiated at 312 nm.

To demonstrate a proof of concept white light emitting device incorporating Tb : Gd : Eu-UiO-66, the MOF was coated onto a UV-LED chip (λ = 310 nm) where the white light emission can be visually observed (Fig. 5c). To test the photostability of Tb : Gd : Eu-UiO-66 under ambient conditions, the MOF was irradiated at 312 nm and emission spectra were collected at 0, 1, 2, 3, 4, 5, and 6 hours (Fig. 6 and Fig. S13, ESI†). Although there are some minor intensity differences observed, in all cases, the blue, green, and red emission bands are maintained, demonstrating that the MOF continues to emit white light for hours under ambient conditions.

Conclusions

In conclusion, the photoluminescent behaviour of RE-UiO-66 has been tuned through the generation of bi-metal and tri-metal Tb : Gd : Eu analogues, ultimately leading to the formation of a white light emitting MOF. The structure and phase purity of all MOFs is confirmed by PXRD and nitrogen adsorption–

desorption analysis with the materials demonstrating high surface area and porosity. The elemental composition of the bi- and tri-metal analogues is determined by ICP-MS while SEM-EDS confirms that the Tb(III), Gd(III), and Eu(III) ions are evenly distributed throughout the MOF crystallites. A ternary system (Tb : Gd : Eu-UiO-66) was found to be necessary for the generation of a white light emitting MOF and single crystals of the tri-metal MOF are observed to emit white light, further confirming that all 3 metal ions are present in individual crystallites. Finally, as a proof of concept, Tb : Gd : Eu-UiO-66 was applied as a surface coating on a UV-LED, giving rise to a device that emits a cool white colour, with no significant photobleaching or photodegradation observed within 6 hours.

Experimental

Synthetic procedures

RE-UiO-66 was synthesized through a solvothermal synthesis where a suspension of $RE(NO_3)_3{\cdot}xH_2O$ (see Table S2 for details, ESI†), terephthalic acid (0.171 mmol, 28.5 mg) and 2,6-difluorobenzoic acid (2.78 mmol, 440 mg) was prepared in 8 mL of DMA in a 6-dram vial. The solution was sonicated until all reagents dissolved and was placed in a 120 °C oven for 72 hours. Once out of the oven, the solution was cooled down to room temperature before centrifugation and subsequent removal of the DMA reaction solvent. The solid material was then washed with fresh DMF (3 × 5 mL) over the course of 24 hours and later with fresh acetone (3 × 5 mL) over the course of 2 days. The material was set to dry in a vacuum oven at 80 °C for 1 hour and was then activated at 120 °C for 20 hours using a Micromeritics Smart VacPrep instrument.

Single crystals of Tb : Gd : Eu-UiO-66 were synthesized through a solvothermal procedure. For that, 0.0798 (35.6 mg), 0.2366 (104 mg), and 0.0246 mmol (10.8 mg) of $Tb(NO_3)_3{\cdot}xH_2O$, $Gd(NO_3)_3{\cdot}xH_2O$, and $Eu(NO_3)_3{\cdot}xH_2O$, respectively, were added to 25 mL of DMA, followed by the addition of formic acid (15 mL), terephthalic acid (0.42 mmol, 70 mg) and 2,6-difluorobenzoic acid (5.69 mmol, 900 mg). After that, the suspension was sonicated until all solids were dissolved and aliquots of 4 mL were distributed in 6-dram vials. The vials were then sealed and placed into a preheated oven at 140 °C for 96 h.

Characterization and photoluminescence data information can be found in the ESI.†

Author contributions

Zvart Ajoyan – conceptualization, methodology, investigation, validation, visualization, writing – original draft; Hudson A. Bicalho – investigation, validation, visualization, project administration, writing – original draft; P. Rafael Donnarumma – conceptualization, investigation, validation; Artsiom Antanovich – investigation, validation; Ashlee J. Howarth – conceptualization, funding acquisition, project administration, resources, supervision, writing – review & editing.

Conflicts of interest

There are no conflicts to declare.

Acknowledgements

The authors thank Prof. Tomislav Friščić for access to X-ray facilities and Dr Vladimir Lesnyak for access and assisting photoluminescence measurements. We acknowledge the support of the Natural Sciences and Engineering Research Council of Canada (NSERC) [funding reference number: RGPIN-2018-04388 (A. J. H.)]. Cette recherche a été financée par le Conseil de recherches en sciences naturelles et en génie du Canada (CRSNG) [numéro de reference: RGPIN-2018-04388 (A. J. H.)]. All structural figures were made using VESTA 3.[66]

Notes and references

1 R. Pode, *Renewable Sustainable Energy Rev.*, 2020, **133**, 110043.
2 D. F. de Souza, P. P. F. da Silva, L. F. A. Fontenele, G. D. Barbosa and M. de Oliveira Jesus, *Energy Rep.*, 2019, **5**, 409–424.
3 A. Bergh, G. Craford, A. Duggal and R. Haitz, *Phys. Today*, 2001, **54**, 42–47.
4 J. Cho, J. H. Park, J. K. Kim and E. F. Schubert, *Laser Photonics Rev.*, 2017, **11**, 1600147.
5 T. Taguchi, *J. Light Visual Environ.*, 2003, **27**, 131–139.
6 P. Pust, P. J. Schmidt and W. Schnick, *Nat. Mater.*, 2015, **14**, 454–458.
7 J. Chen, S. Mukherjee, W. Li, H. Zeng and R. A. Fischer, *Nat. Rev. Mater.*, 2022, **7**, 677–678.
8 A. Mills, *III-Vs rev.*, 2005, **18**, 32–34.
9 S. Tabuchi, *Japanese Utility Model Patent Application*, Publication No. S50-79379, 1973.
10 Y. Shimizu, *Japanese Patent Application*, Publication No. H08-7614, 1996.
11 C. S. McCamy, *Color Res. Appl.*, 1992, **17**, 142–144.
12 Y. Yang, M. Lowry, C. M. Schowalter, S. O. Fakayode, J. O. Escobedo, X. Xu, H. Zhang, T. J. Jensen, F. R. Fronczek, I. M. Warner and R. M. Strongin, *J. Am. Chem. Soc.*, 2006, **128**, 14081–14092.
13 S. Mukherjee and P. Thilagar, *Dyes Pigm.*, 2014, **110**, 2–27.
14 Y. Yang, L. Chen, F. Jiang, M. Yu, X. Wan, B. Zhang and M. Hong, *J. Mater. Chem. C*, 2017, **5**, 1981–1989.
15 Y. Wang, J. Ding, Y. Wang, X. Zhou, Y. Cao, B. Ma, J. Li, X. Wang, T. Seto and Z. Zhao, *J. Mater. Chem. C*, 2019, **7**, 1792–1820.
16 P. Coppo, M. Duati, V. N. Kozhevnikov, J. W. Hofstraat and L. De Cola, *Angew. Chem., Int. Ed.*, 2005, **44**, 1806–1810.
17 M. J. Bowers, J. R. McBride and S. J. Rosenthal, *J. Am. Chem. Soc.*, 2005, **127**, 15378–15379.
18 Y. Hu, X. Liang, D. Wu, B. Yu, Y. Wang, Y. Mi, Z. Cao and Z. Zhao, *J. Mater. Chem. C*, 2020, **8**, 734–741.
19 J. Cornil, D. Beljonne, J. P. Calbert and J. L. Brédas, *Adv. Mater.*, 2001, **13**, 1053–1067.

20 F. So, J. Kido and P. Burrows, *MRS Bull.*, 2008, **33**, 663–669.
21 B. F. Hoskins and R. Robson, *J. Am. Chem. Soc.*, 1990, **112**, 1546–1554.
22 H. Li, M. Eddaoudi, M. O'Keeffe and O. M. Yaghi, *Nature*, 1999, **402**, 276–279.
23 M. Kondo, T. Yoshitomi, H. Matsuzaka, S. Kitagawa and K. Seki, *Angew. Chem., Int. Ed. Engl.*, 1997, **36**, 1725–1727.
24 F. Serpaggi and G. Férey, *J. Mater. Chem.*, 1998, **8**, 2737–2741.
25 O. M. Yaghi and H. Li, *J. Am. Chem. Soc.*, 1995, **117**, 10401–10402.
26 O. M. Yaghi, G. Li and H. Li, *Nature*, 1995, **378**, 703–706.
27 M.-S. Wang, S.-P. Guo, Y. Li, L.-Z. Cai, J.-P. Zou, G. Xu, W.-W. Zhou, F.-K. Zheng and G.-C. Guo, *J. Am. Chem. Soc.*, 2009, **131**, 13572–13573.
28 M.-S. Wang, G.-C. Guo, W.-T. Chen, G. Xu, W.-W. Zhou, K.-J. Wu and J.-S. Huang, *Angew. Chem., Int. Ed.*, 2007, **46**, 3909–3911.
29 D. F. Sava, L. E. S. Rohwer, M. A. Rodriguez and T. M. Nenoff, *J. Am. Chem. Soc.*, 2012, **134**, 3983–3986.
30 J. He, M. Zeller, A. D. Hunter and Z. Xu, *J. Am. Chem. Soc.*, 2012, **134**, 1553–1559.
31 C.-Y. Sun, X.-L. Wang, X. Zhang, C. Qin, P. Li, Z.-M. Su, D.-X. Zhu, G.-G. Shan, K.-Z. Shao, H. Wu and J. Li, *Nat. Commun.*, 2013, **4**, 2717.
32 C. Peng, X. Song, J. Yin, G. Zhang and H. Fei, *Angew. Chem., Int. Ed.*, 2019, **58**, 7818–7822.
33 L. Qiu, C. Yu, X. Wang, Y. Xie, A. M. Kirillov, W. Huang, J. Li, P. Gao, T. Wu, X. Gu, Q. Nie and D. Wu, *Inorg. Chem.*, 2019, **58**, 4524–4533.
34 N.-C. Chiu, K. T. Smith and K. C. Stylianou, *Coord. Chem. Rev.*, 2022, **459**, 214441.
35 S. Dang, J.-H. Zhang and Z.-M. Sun, *J. Mater. Chem.*, 2012, **22**, 8868–8873.
36 K. Liu, H. You, Y. Zheng, G. Jia, Y. Huang, M. Yang, Y. Song, L. Zhang and H. Zhang, *Cryst. Growth Des.*, 2010, **10**, 16–19.
37 R. Peña-Rodríguez, J. A. Molina-González, H. Desirena-Enrriquez, E. Armenta-Jaime, J. M. Rivera and S. E. Castillo-Blum, *J. Mater. Chem. C*, 2021, **9**, 15891–15899.
38 L. H. Slooff, A. Polman, S. I. Klink, L. Grave, F. C. J. M. van Veggel and J. W. Hofstraat, *J. Opt. Soc. Am. B*, 2001, **18**, 1690–1694.
39 H. A. Bicalho, F. Saraci, J. D. J. Velazquez-Garcia, H. M. Titi and A. J. Howarth, *Chem. Commun.*, 2022, **58**, 10925–10928.
40 Y. Wang, K. Zhang, X. Wang, X. Xin, X. Zhang, W. Fan, B. Xu, F. Dai and D. Sun, *J. Mater. Chem. C*, 2020, **8**, 1374–1379.
41 F. Saraci, V. Quezada-Novoa, P. R. Donnarumma and A. J. Howarth, *Chem. Soc. Rev.*, 2020, **49**, 7949–7977.
42 A. Dhakshinamoorthy, A. Santiago-Portillo, A. M. Asiri and H. Garcia, *ChemCatChem*, 2019, **11**, 899–923.
43 A. Shaabani, R. Mohammadian, S. E. Hooshmand, A. Hashemzadeh and M. M. Amini, *ChemistrySelect*, 2017, **2**, 11906–11911.
44 Y. Jiao, Y. Liu, G. Zhu, J. T. Hungerford, S. Bhattacharyya, R. P. Lively, D. S. Sholl and K. S. Walton, *J. Phys. Chem. C*, 2017, **121**, 23471–23479.
45 S. Chavan, J. G. Vitillo, D. Gianolio, O. Zavorotynska, B. Civalleri, S. Jakobsen, M. H. Nilsen, L. Valenzano, C. Lamberti, K. P. Lillerud and S. Bordiga, *Phys. Chem. Chem. Phys.*, 2012, **14**, 1614–1626.
46 X. Yang, Z. Li and S. Tang, *Cryst. Growth Des.*, 2021, **21**, 6092–6100.
47 P. R. Donnarumma, S. Frojmovic, P. Marino, H. A. Bicalho, H. M. Titi and A. J. Howarth, *Chem. Commun.*, 2021, **57**, 6121–6124.
48 M. H. V. Werts, R. T. F. Jukes and J. W. Verhoeven, *Phys. Chem. Chem. Phys.*, 2002, **4**, 1542–1548.
49 G. Deng, *Nat. Chem.*, 2018, **10**, 110.
50 D. Briones, P. Leo, J. Cepeda, G. Orcajo, G. Calleja, R. Sanz, A. Rodríguez-Diéguez and F. Martínez, *CrystEngComm*, 2018, **20**, 4793–4803.
51 T. Tachikawa, J. R. Choi, M. Fujitsuka and T. Majima, *J. Phys. Chem. C*, 2008, **112**, 14090–14101.
52 S. Bordiga, C. Lamberti, G. Ricchiardi, L. Regli, F. Bonino, A. Damin, K. P. Lillerud, M. Bjorgen and A. Zecchina, *Chem. Commun.*, 2004, 2300–2301.
53 J.-K. Cheng, P.-X. Yin, Z.-J. Li, Y.-Y. Qin and Y.-G. Yao, *Inorg. Chem. Commun.*, 2007, **10**, 808–810.
54 W. Chen, J.-Y. Wang, C. Chen, Q. Yue, H.-M. Yuan, J.-S. Chen and S.-N. Wang, *Inorg. Chem.*, 2003, **42**, 944–946.
55 H.-Q. Yin, X.-Y. Wang and X.-B. Yin, *J. Am. Chem. Soc.*, 2019, **141**, 15166–15173.
56 Z. Ajoyan, G. A. Mandl, P. R. Donnarumma, V. Quezada-Novoa, H. A. Bicalho, H. M. Titi, J. A. Capobianco and A. J. Howarth, *ACS Mater. Lett.*, 2022, 1025–1031.
57 J. P. Vizuet, M. L. Mortensen, A. L. Lewis, M. A. Wunch, H. R. Firouzi, G. T. McCandless and K. J. Balkus, *J. Am. Chem. Soc.*, 2021, **143**, 17995–18000.
58 X. Song, Q. Huang, J. Liu, H. Xie, K. B. Idrees, S. Hou, L. Yu, X. Wang, F. Liu, Z. Qiao, H. Wang, Y. Chen, Z. Li and O. K. Farha, *ACS Appl. Mater. Interfaces*, 2023, **15**, 18229–18235.
59 D. Parker, *Coord. Chem. Rev.*, 2000, **205**, 109–130.
60 M. Latva, H. Takalo, V.-M. Mukkala, C. Matachescu, J. C. Rodríguez-Ubis and J. Kankare, *J. Lumin.*, 1997, **75**, 149–169.
61 Y. Zhang, W. Thor, K.-L. Wong and P. A. Tanner, *J. Phys. Chem. C*, 2021, **125**, 7022–7033.
62 M. W. Mara, D. S. Tatum, A.-M. March, G. Doumy, E. G. Moore and K. N. Raymond, *J. Am. Chem. Soc.*, 2019, **141**, 11071–11081.
63 A. N. Carneiro Neto, R. T. Moura, A. Shyichuk, V. Paterlini, F. Piccinelli, M. Bettinelli and O. L. Malta, *J. Phys. Chem. C*, 2020, **124**, 10105–10116.
64 H. Li, H.-B. Liu, X.-M. Tao, J. Su, P.-F. Ning, X.-F. Xu, Y. Zhou, W. Gu and X. Liu, *Dalton Trans.*, 2018, **47**, 8427–8433.
65 I. Carrasco, F. Piccinelli and M. Bettinelli, *J. Lumin.*, 2017, **189**, 71–77.
66 K. Momma and F. Izumi, *J. Appl. Crystallogr.*, 2011, **44**, 1272–1276.

